

# Cloning and Characterization of *GLOSSY1*, a Maize Gene Involved in Cuticle Membrane and Wax Production<sup>1[w]</sup>

Monica Sturaro, Hans Hartings, Elmon Schmelzer, Riccardo Velasco, Francesco Salamini, and Mario Motto\*

Istituto Sperimentale per la Cerealicoltura, Sezione di Bergamo, 24126 Bergamo, Italy (M.S., H.H., M.M.); and Max-Planck Institut für Züchtungsforschung, D-50829 Cologne, Germany (E.S., R.V., F.S.)

The cuticle covering the aerial organs of land plants plays a protective role against several biotic and abiotic stresses and, in addition, participates in a variety of plant-insect interactions. Here, we describe the molecular cloning and characterization of the maize (*Zea mays*) *GLOSSY1* (*GL1*) gene, a component of the pathway leading to cuticular wax biosynthesis in seedling leaves. The genomic and cDNA sequences we isolated differ significantly in length and in most of the coding region from those previously identified. The predicted *GL1* protein includes three histidine-rich domains, the landmark of a family of membrane-bound desaturases/hydroxylases, including fatty acid-modifying enzymes. *GL1* expression is not restricted to the juvenile developmental stage of the maize plant, pointing to a broader function of the gene product than anticipated on the basis of the mutant phenotype. Indeed, in addition to affecting cuticular wax biosynthesis, *gl1* mutations have a pleiotropic effect on epidermis development, altering trichome size and impairing cutin structure. Of the many wax biosynthetic genes identified so far, only a few from *Arabidopsis* (*Arabidopsis thaliana*) were found to be essential for normal cutin formation. Among these is *WAX2*, which shares 62% identity with *GL1* at the protein level. In *wax2*-defective plants, cutin alterations induce postgenital organ fusion. This trait is not displayed by *gl1* mutants, suggesting a different role of the maize and *Arabidopsis* cuticle in plant development.

The cuticle forms the outermost layer of the above-ground parts of most plants. The physical and chemical properties of this structure support vital functions such as prevention of nonstomatal water loss, protection against UV irradiation, and reduction of deposition of dust, pollen, and air pollutants. In addition, it plays a critical role in plant defense against bacterial and fungal pathogens and participates in a variety of plant-insect interactions (Post-Beittenmiller, 1996).

The cuticle is synthesized by the epidermal cells and consists of an outer layer of epicuticular waxes overlaying the cuticle membrane, which is composed of a network of interesterified hydroxy and epoxy-hydroxy fatty acids of mainly 16 and 18 atoms in length (cutin) interspersed by intracuticular waxes (Walton, 1990). Cuticular waxes consist primarily of complex mixtures of aliphatic molecules of mainly 16 to 34 carbon atoms in length that occur as free fatty acids, aldehydes, primary alcohols, alkanes, and esters. Their production is a biologically complex process involving a host of synthetic and transport mechanisms. The composition of cuticular waxes differs among plant species, organs, and tissues, and during development. Wax deposition on the leaf surface is also regulated by

environmental signals such as light, moisture, and temperature (Kolattukudy, 1996).

Although advances have been made in the understanding of the biosynthesis of specific cutin and wax constituents, many questions pertaining to the organization and regulation of the concerned biochemical pathways remain unanswered. The availability of mutants deficient in cuticular wax accumulation in a variety of species and the isolation of the corresponding genes reveal helpful information to elucidate cuticular wax biosynthesis and to characterize molecular aspects of regulatory control (Kunst and Samuels, 2003).

In maize (*Zea mays*), at least 18 loci (the *GLOSSY* or *GL* loci) have been found to affect the quantity and/or the composition of cuticular waxes on the surface of seedling leaves (Neuffer et al., 1997). From genetic and biochemical analyses of maize plants carrying different *gl* mutations, a preliminary model predicting two distinct pathways for cuticular wax biosynthesis has been set forth (Bianchi et al., 1985). One pathway would be responsible for wax synthesis in the first five or six juvenile leaves, whereas the other would produce waxes during the whole life cycle of the maize plant. The products of these two pathways can be distinguished by their chemical composition: Approximately 80% of the juvenile waxes are very-long-chain alcohols and aldehydes, whereas approximately 70% of the waxes produced throughout the life of a maize plant consist of esters (Bianchi et al., 1985). These ontogenetic differences in wax composition lead to different phenotypes of the maize leaves; juvenile

<sup>1</sup> This work was supported by grants from the Ministero delle Politiche Agricole e Forestali, Rome.

\* Corresponding author; e-mail motto@iscbg.it; fax 39-035-31-60-54.

<sup>[w]</sup> The online version of this article contains Web-only data.

Article, publication date, and citation information can be found at [www.plantphysiol.org/cgi/doi/10.1104/pp.104.058164](http://www.plantphysiol.org/cgi/doi/10.1104/pp.104.058164).

leaves of wild-type maize plants have a glaucous surface appearance, whereas all leaves appearing later in plant development have a glossy surface. Mutations impairing the juvenile wax pathway also confer a glossy appearance to the juvenile leaves. Because of their phenotypic appearance, such mutants were designated *glossy*. The different composition of the wax layer of epidermal cells of juvenile and adult leaves is one of the traits that defines the juvenile-to-adult phase transition in wild-type maize plants (Lawson and Poethig, 1995, and refs. therein).

Over the past years, various maize *GLOSSY* genes involved in cuticular wax production have been cloned (Moose and Sisco, 1994; Tacke et al., 1995; Hansen et al., 1997; Xu et al., 1997). Based on evidence presented by Xu et al. (2002), *GL8* encodes as a  $\beta$ -ketoacyl reductase of the fatty acid elongase complex involved in wax production. *GL2* is apparently involved in acyl chain elongation from C30 to C32. However, comparisons of the predicted *GL2* sequence with those in protein databases revealed no similarities to any known fatty acyl synthases, as may be expected for a component of the acyl elongation pathway (Tacke et al., 1995). The *GL15* locus is a developmental gene belonging to the *APETALA2* family of regulatory genes involved in the transition from juvenile to adult leaves (Moose and Sisco, 1996). The glossy phenotype of *gl15* mutants is secondary to the primary mutant defect supporting the precocious development of adult leaves.

Mutation at the *GL1* locus causes dramatic alterations in the amount, composition, and crystallization patterns of juvenile cuticular waxes (Bianchi et al., 1985). The most conspicuous property of *gl1* waxes, in addition to a large reduction of aldehydes and alcohols, concerns the predominant chain length of long-chain aldehydes and the corresponding free and esterified alcohols, which turn out to be reduced by two carbon atoms. In this context, it has been hypothesized that the *GL1* locus is either required for an elongation step in cuticular wax biosynthesis or is affecting the supply of wax precursors. However, the specific role of *GL1* that emerged from these chemical studies was neither precise nor definitive.

In an effort to characterize the *Gl1* gene, we performed transposon-tagging experiments with the *Enhancer/Suppressor mutation (En/Spm)* element, which led to the tagging of the *GL1* locus (Maddaloni et al., 1990). In this article, we describe the cloning and molecular characterization of this gene. The genomic and cDNA sequences we have isolated differ in most of the coding region from the putative *GL1* gene and transcript previously identified by Hansen et al. (1997). The protein encoded by *GL1* shows significant homology with the entire sequence of the *WAX2* gene product of *Arabidopsis thaliana* involved in both cutin development and cuticular wax production (Chen et al., 2003). Similarly, the *gl1* mutant displays a reduction in cuticular wax deposition and an alteration in cuticle membrane and plant hair (trichome) morphology.

## RESULTS

### Isolation of Transposon-Tagged Alleles of the *GL1* Locus

From the cross outlined in "Materials and Methods," nine glossy seedlings with revertant nonglossy sectors were identified out of approximately 90,000  $F_1$  seedlings. The new alleles were designated *gl1-m1* through *gl1-m9*. Genetic analyses of the new mutable alleles are described by Maddaloni et al. (1990). Seven alleles, *gl1-m1*, 2, 3, 5, 7, 8, and 9, are due to the insertion of an element behaving autonomously but, contrary to expectation, are different from *Activator (Ac)*. The alleles *gl1-m4* and *-m6* carried a nonautonomous element.

Plants carrying the *gl1-m5* allele were tested for the functional presence in their genome of the transposable element *En/Spm*. Plants heterozygous for the *gl1-m5* allele and for the stable recessive reference allele *gl1-ref* were crossed with the *En/Spm* tester strains described in "Materials and Methods." Three independent test crosses were performed.  $F_1$  plants of each test cross were selfed, and the resulting ears were scored for  $F_2$  kernels displaying reversions of the *a1-m1* or *a1-m(r)* tester allele. All three groups of  $F_1$  plants gave rise to segregating and nonsegregating ears, with a percentage of the former near to 75%, suggesting the presence, in the *gl1-m5* progenitor, of two unlinked copies of an active *En/Spm* element.  $F_2$  kernels of both groups of ears were grown to seedlings, and these were scored for leaf variegation due to the *gl1-m5* allele. The results of these experiments are summarized in Table I. Approximately one-half of the ears that segregated for variegated kernels also segregated *gl1-m5* variegated seedlings, while ears without variegated seeds did not originate variegated seedlings. This result indicates that the *gl1-m5* allele is likely to be caused by the insertion of an autonomous active *En/Spm* element.

### Phenotypic Analysis of *gl1* Mutants

Morphology of epicuticular waxes of wild-type and *gl1* plants was previously examined with scanning electron microscopy (SEM) by Lorenzoni and Salamini (1975). This study showed that epidermal cells of *gl1* seedling leaves are almost waxless, except for stomata

**Table I.** Genetic test for the presence of *En/Spm* in the *gl1-m5* strain

Cross	Segregation			
	F <sub>2</sub> Ears with Variegated Kernels		F <sub>2</sub> Ears without Variegated Kernels	
	<i>gl1-m5</i>	<i>gl1-ref</i>	<i>gl1-m5</i>	<i>gl1-ref</i>
1	4	3	0	3
2	5	4	0	4
3	5	6	0	4
Total	14	13	0	11

subsidiary cells and cells of the leaf borders. Wax extrusion on *gl1* leaves is reduced in size and has a round shape in contrast to the crystalline microstructure of wild-type epicuticular wax.

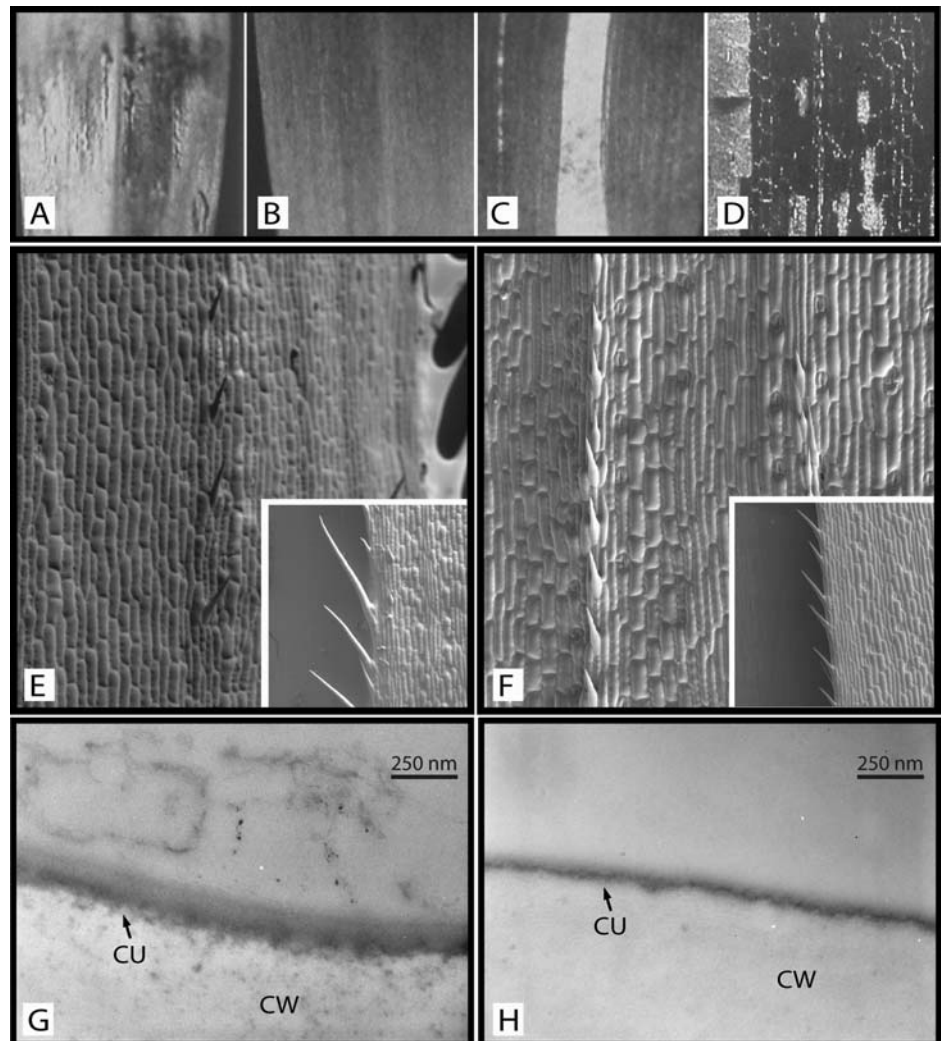
The wax phenotypes of a *GL1* wild-type allele, of the recessive *gl1-ref* allele and of the unstable *gl1-m5* allele are shown in Figure 1, A to C, as revealed by visual and microscopic inspections. The *gl1-m5* allele shows clear somatic instability that is visible as sectors of wild-type tissue in a mutant background (Fig. 1D). The revertant sectors can cover small or large parts of a leaf (up to one-half) or are restricted to single epidermal cells. This finding shows that *GL1*, like other *GL* genes, acts cell autonomously during juvenile leaf development (Moose and Sisco, 1994; Tacke et al., 1995).

Epidermal cells of maize leaves are arranged in cell rows that extend longitudinally parallel with the veins and show a gradient of cell differentiation from the leaf base to the leaf tip. Selected cell rows are enriched with stomata, others with trichomes, while still others are devoid of both types of specialized epidermal cells.

*gl1* mutant trichomes are smaller and more closely spaced in comparison to the wild type. In the apical region of fully developed juvenile leaves, their size is about one-half that of the wild type; on the leaf margin, mean distance between mutant and wild-type trichomes is  $124 \pm 14 \mu\text{m}$  and  $171 \pm 28 \mu\text{m}$ , respectively (Fig. 1, E and F). Stomata distribution on *gl1* leaves does not differ from the wild type.

Ultrastructural analysis of the leaf cuticle with transmission electron microscopy (TEM) indicates that the wild-type cuticle membrane appears to be divided into an outermost translucent layer (the cuticle proper) and an innermost opaque layer (the reticulated cuticular layer; Fig. 1G). In the *gl1* mutant, cuticle membrane thickness is clearly reduced by about 50% and the cuticle proper appears almost absent (Fig. 1H). No differences in permeability to chlorophyll were detected in *gl1* leaves compared to the wild type, as determined with extraction in 80% ethanol, with or without prior removal of cuticular waxes (data not shown). *gl1* plants do not show reduction in pollen

**Figure 1.** The leaf surface in wild-type and *gl1* alleles. Phenotype of a wild-type allele at the *GL1* locus (A) compared to a stable recessive (B) and a mutable (C) allele, as seen when under water. D, Phenotype seen on the abaxial surface of the second leaf viewed with SEM: The reverted cells appear white in a dark background. SEM analysis of wild-type (E) and mutant (F) leaf surfaces. Insets, Close-up view of upper surface showing details of trichome morphology and density (all images are at  $100\times$  enlargement). TEM analysis of wild-type (G) and mutant (H) cuticle membranes is shown. CU, Cuticle; CW, cell wall.



fertility, probably because waxes affected by the mutation are those found on juvenile leaves.

### Isolation and Characterization of the *gl1-m5* Allele

The internal *EcoRI/BamHI* fragment of the *En/Spm* element was used as a hybridization probe in DNA gel-blot analyses of families segregating for *gl1-m5*. An 8.3-kb *HindIII* fragment that cosegregated with the *gl1-m5* mutant phenotype was identified. Representative homozygous (lanes 4 and 5) and heterozygous (lanes 6 and 7) *gl1-m5* plants with the 8.3-kb *En/Spm* hybridizing fragment are shown in Figure 2A. Evidence that the *HindIII* fragment represents an *En/Spm* insertion in the *GL1* gene came from the absence of this fragment in plants homozygous for germinal reverted alleles derived from *gl1-m5* (Fig. 2A, lanes 2 and 3). No other *En/Spm* hybridizing fragments from *gl1-m5* plants were consistently found to be missing from these derivatives.

A size-fractionated subgenomic library of *HindIII* fragments from heterozygous *gl1-m5* plants was constructed in the  $\lambda$ EMBL3 vector, and the 8.3-kb *HindIII* fragment was isolated in the clone  $\lambda$ -09 using the *EcoRI/BamHI* probe of the *En/Spm* element. The restriction map of the cloned *HindIII* fragment indicated the presence of an *En/Spm* element flanked by non-*En/Spm* sequences. A restriction fragment (0.95-kb *HindIII-XhoI*) carried by the non-*En/Spm* sequence was used as a hybridization probe to the same DNA gel blot shown in Figure 2A. The resulting hybridization pattern is shown in Figure 2B. Homozygous *gl1-m5* plants, which exhibit an unstable phenotype in the presence of the autonomous *En/Spm*, showed the expected 8.3-kb *HindIII* fragment and a low-intensity 6.0-kb fragment (lanes 4 and 5). The 6.0-kb fragment was correlated with the generation of somatic revertant sectors from *gl1-m5* and thus represented the original progenitor allele. Proof that the 0.95-kb *HindIII-XhoI* fragment represents part of the *GL1* gene came from comparing the two independent germinal revertant derivatives of *gl1-m5* (lanes 2 and 3) with their mutable siblings (lanes 4–7). The homozygous revertant plants contained only a 6.0-kb *HindIII* hybridizing fragment, whereas their mutable siblings heterozygous for the *gl1-m5* and *gl1-ref* alleles, contained the 8.3- and 6.0-kb fragments (lanes 6 and 7). The size difference between the restriction fragment representing *gl1-m5* and its somatic and germinal revertant derivatives was consistent with the *En/Spm* insertion observed within the cloned 8.3-kb *HindIII* fragment (Fig. 2B).

Although these results indicated that  $\lambda$ -09 contains a DNA fragment cosegregating with the *gl1-m5* allele, they did not unambiguously establish that this clone was derived from the *GL1* locus. To establish whether the DNA fragment in clone  $\lambda$ -09 indeed represented the *GL1* locus, the 0.95-kb *HindIII-XhoI* fragment of this clone was used as a hybridization probe in allelic

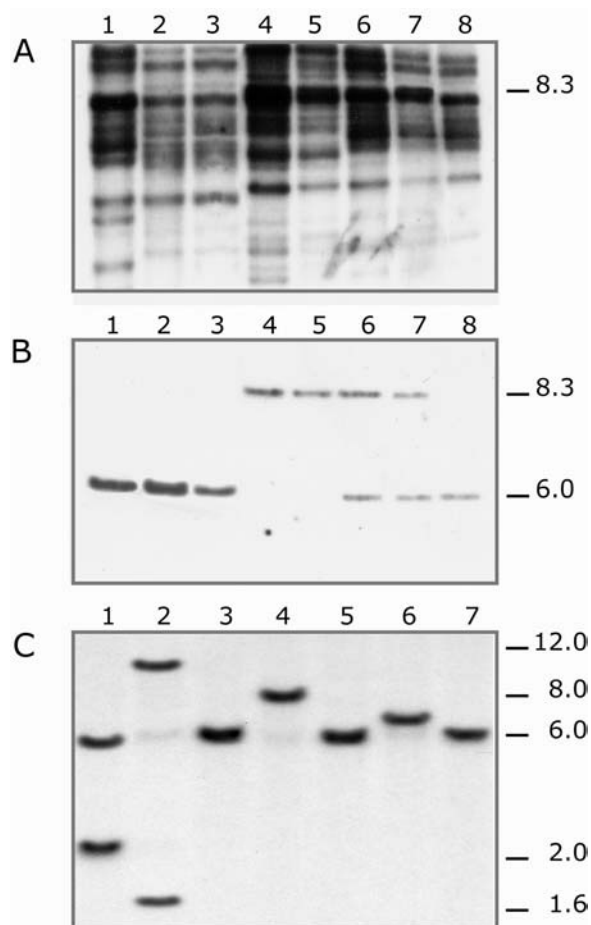


**Figure 2.** Southern analysis of the *gl1-m5* locus and other mutable alleles. Maize DNA cleaved with *HindIII* was subjected to Southern hybridization. The *EcoRI/BamI* fragment spanning the region between positions 2,518 to 4,459 of the *En/Spm* element and the 0.95-kb *HindIII-XhoI* *gl1-m5*-derived fragments were used as a probe in A and B, respectively. Alleles are designed as follows: (1) wild-type allele from the inbred line WF9; (2) *GL1-Rev2* and (3) *GL1-Rev3*; revertant alleles obtained from *gl1-m5*; (4 and 5) homozygous *gl1-m5* plants; (6 and 7) plants heterozygous for *gl1-m5* and *gl1-ref* showing a *gl1* mutable phenotype; and (8) homozygous *gl1-ref* plants. A, The 8.3-kb band characteristic of the *gl1-m5* allele is absent in revertant derivatives of *gl1-m5*. B, The blot in A was stripped and rehybridized with an *HindIII-XhoI* probe derived from *gl1-m5*. The 8.3-kb *HindIII* fragment from the *gl1-m5* allele and the 6.0-kb fragment from the *GL1-Wf9* and either *gl1-m5* revertant or the *gl1-ref* alleles are indicated. C, Allelic cross-referencing experiments. DNA isolated from plants that carried the seven unstable mutant alleles *gl1-m1* (1), *-m2* (2), *-m3* (3), *-m5* (4), *-m7* (5), *-m8* (6), and *-m9* (7) was digested with *HindIII*, electrophoresed on agarose gel, and transferred to a nylon membrane. Hybridization with the 0.95-kb *HindIII-XhoI* fragment of  $\lambda$ -09 revealed polymorphism associated with the *gl1-m5* allele relative to other *gl1 En/Spm* mutable alleles. Molecular sizes (kb) are indicated.

cross-reference experiments. The rationale for these experiments was that if this probe derives from the *GL1* locus, then it should detect RFLPs between unstable *gl1* mutants and their respective wild-type alleles. Southern-blot analyses were performed on DNA from seven independent *gl1* mutable alleles

(each of which carried an independently derived *gl1 En/Spm* allele). Hybridization with the 0.95-kb *HindIII-XhoI* fragment from  $\lambda$ -09 revealed a fragment of different size according to the specific allelic state of the *GL1* locus (Fig. 2C). All indications obtained from the Southern experiments strongly suggested that the probe used for hybridization was able to recognize allelic states modifying, at the molecular level, the *GL1* locus. It was concluded that the 0.95-kb *HindIII-XhoI* DNA sequences isolated from clone  $\lambda$ -09 mark a specific tract of the maize genome that corresponds to the *GL1* locus.

### Sequence Analysis of the *GL1* Locus

The *HindIII-XhoI* fragment derived from clone  $\lambda$ -09 was used as a molecular probe in hybridization experiments on a maize bacterial artificial chromosome (BAC) library derived from inbred line F<sub>2</sub>. Twenty-three independent clones were identified, eight of which were subsequently analyzed by restriction mapping. Two adjacent *HindIII* fragments, one of which hybridized with the molecular probe derived from clone  $\lambda$ -09, could be identified in all clones considered and were used to obtain the nucleotide sequence of the entire *GL1* locus together with a 2.1-kb promoter fragment.

Computer-aided analysis of the genomic sequence obtained identified the putative exons encompassing the *GL1* transcript. A database search for proteins homologous to the deduced *GL1* polypeptide bolstered the postulated mRNA sequence. On the basis of these data, two primers were designed to isolate the full-length coding sequence of *GL1* by reverse transcription (RT)-PCR. A single 2,056-bp fragment, including a 1,866-nucleotide-long open reading frame (ORF), was amplified from RNA extracted from wild-type seedling leaves of the inbred Wf9. From a partial cDNA clone isolated from a seedling cDNA library, we deduced that the *GL1* transcript contains a 240-bp-long untranslated region (UTR) at its 3' end (data not

shown). The 5' UTR was previously found to be 185 bp long. Taken together, these data suggest an approximate length of 2,291 bp for the *GL1* transcript. An in-frame stop codon was present 87 bp upstream of the ATG start codon of the main ORF. No alternative translation start sites were present, indicating that the amplified fragment included the complete coding region. Putative CAAT- and TATA-box motifs were found in the promoter sequence 200 and 146 bp upstream of the ATG start codon, respectively, while a putative polyadenylation site was present 312 bp downstream of the translation stop codon.

Alignment of cDNA and genomic sequences revealed the presence of eight noncontiguous stretches of homology, interspersed with seven intron sequences ranging in size from 95 to 2,025 bp (Fig. 3). The deduced coding sequence displays three single base differences with respect to the genomic sequence considered. This discrepancy is due to polymorphism between the two strains used for the isolation of genomic and cDNA clones, as confirmed by sequence analysis of the corresponding genomic regions of the Wf9 inbred line (data not shown).

### Mapping of *En/Spm* Insertion Sites

The available unstable *gl1* alleles were examined by Southern analysis using different fragments of the *GL1* gene as probes. All unstable alleles were found to be caused by independent insertions of members of the *En/Spm* transposable element family. The approximate insertion site and the orientation of the elements with respect to the *GL1* gene were determined for all seven unstable alleles. In four cases (*gl1-m1*, 2, 5, and 8), the transposable element was inserted distal to the *HindIII* restriction site present in the fourth intron of the *GL1* locus, which has been used previously to delimit the end of the *GL1* gene (Fig. 3; Hansen et al., 1997).

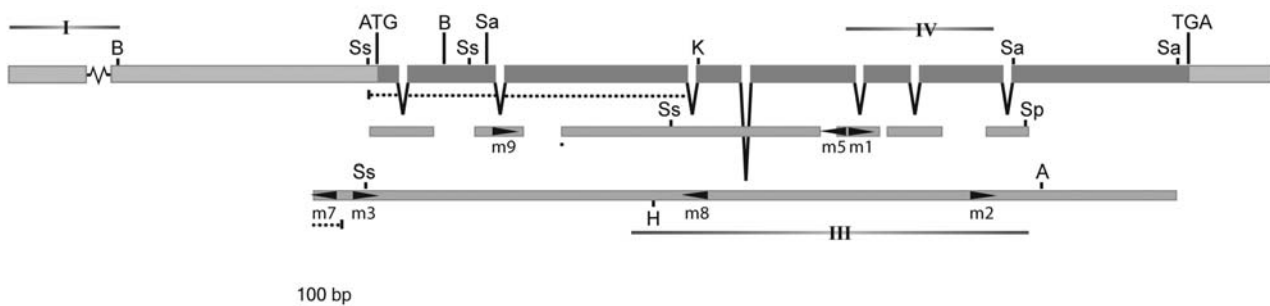


**Figure 3.** Molecular map of the *GL1* locus. Exon sequences (top line) together with interspersing intron sequences (middle and bottom lines) are reported. The approximate position of insertion sites of *En/Spm* transposable element sequences present in *gl1* mutable alleles (*m1*–*m9*) is indicated with arrowheads indicating transposable element orientation. ATG start and TGA stop codons, as well as restriction sites of the *ApaI* (A), *BamHI* (B), *HindIII* (H), *KpnI* (K), *Sall* (Sa), *SpeI* (Sp), and *SstI* (Ss) endonucleases are reported. DNA segments used as molecular probes in Southern analyses are indicated and marked I, III, and IV. Probe II, consisting of an *SstI* (intron 3)–*SstI* (intron 4) fragment, is not indicated.

The identification of the transposable elements present at the different unstable *gl1* alleles and the location of the insertion point in the known sequence of the *GL1* gene made possible a PCR-mediated amplification of specific fragments spanning the 5' and 3' junctions between the *gl1* and terminal transposable element sequences. *GL1*- and *En/Spm*-specific primers were employed in PCR amplification reactions (see Supplemental Tables II and III) generating amplified fragments of the expected lengths. All amplification products were sequenced to determine the precise insertion point of the transposable element present in each of the unstable *gl1* alleles (Fig. 3). The seven *En/Spm* insertions are all placed within the genomic region encompassed by the cDNA sequence. In all cases, the characteristic target site duplication of three nucleotides for *En/Spm* was observed (data not shown).

### Characterization of the Predicted GL1 Protein

Conceptual translation of the 1,866-nucleotide-long ORF present in the *GL1* cDNA sequence gave rise to a putative polypeptide of 621 amino acids with an apparent molecular mass of 69.6 kD and a pI of 9.89.

Hydropathy analysis predicted the presence of several transmembrane domains in the N-terminal region of the GL1 polypeptide, as well as of a hydrophilic C-terminal domain. Furthermore, a tripartite His-rich motif characteristic of a family of membrane-bound desaturases/hydroxylases was present in the N-terminal part.

Compared to our cDNA, the sequence previously identified as the *GL1* transcript by Hansen et al. (1997) is shorter and differentially spliced. In particular, it includes the first four exons of our cDNA and two stretches of intervening sequences: four bases of the third intron and 533 bases of the fourth intron. The former base insertion changes the reading frame and leads to the suppression of the third His-rich motif in the putative polypeptide (Fig. 4).

A database search for proteins homologous to GL1 with the TBLASTX algorithm revealed several sequences exhibiting high levels of similarity with the query sequence used. In particular, a putative polypeptide of 619 amino acids encoded by a cDNA from rice (*Oryza sativa*; AK060786) showed 84% identity over its entire coding sequence. Furthermore, significant homologies, with a 67% identity score, were found with

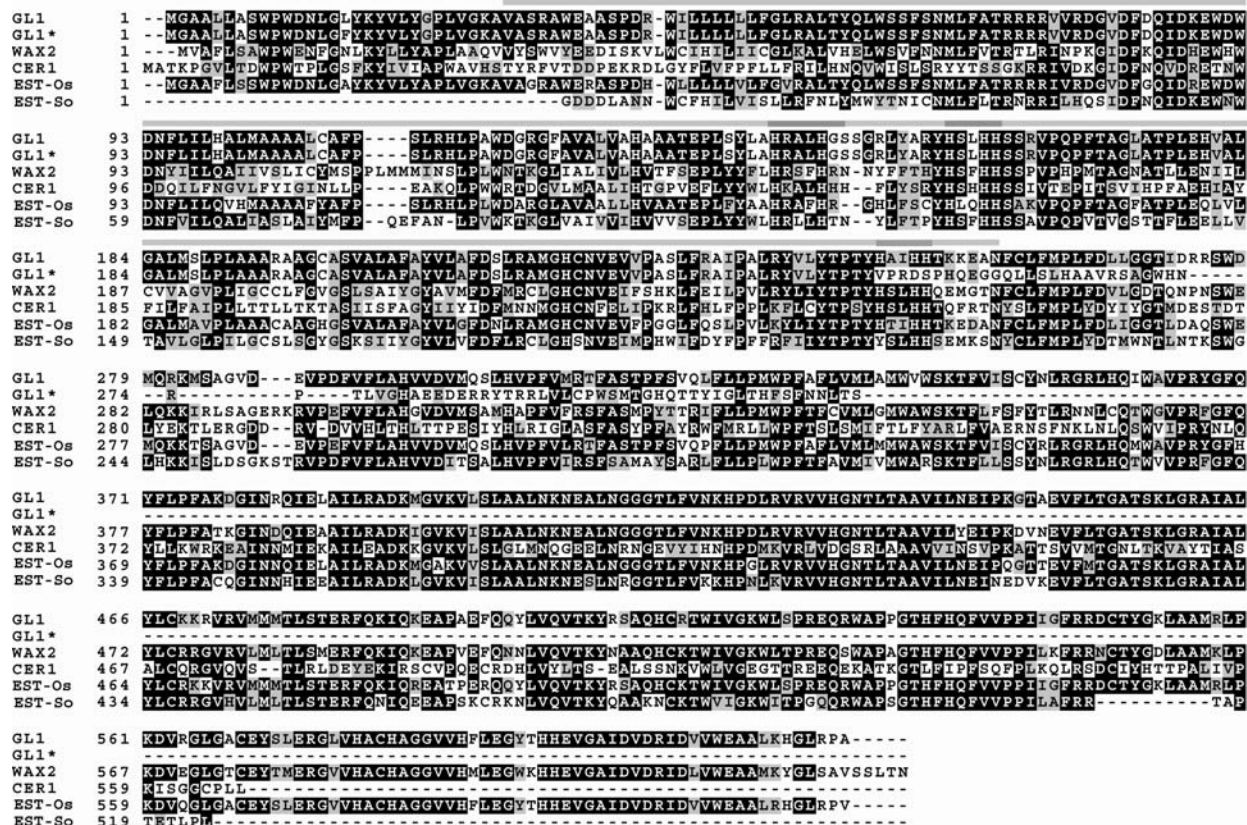


**Figure 4.** Alignment of *GL1* homologous sequences. The GL1 protein sequence (top line) was aligned against the polypeptides encoded by Hansen's cDNA (GL1\*), Arabidopsis At5g57800 (WAX2), Arabidopsis At1g02205 (CER1), rice AK060786.1 (EST-Os), and *S. odorus* L33792 (EST-So). Identical residues are boxed in black and similar residues in gray. The conserved desaturase/hydroxylase domain is marked above the GL1 sequence with a gray line. Darker gray segments identify conserved His residues within the desaturase/hydroxylase domain.

the products of two other rice cDNAs (AK066569 and AK070469), with the *WAX2* locus of Arabidopsis encoding a protein involved in cuticle synthesis (62% identity), and a partial polypeptide (L33792) derived from *Senecio odorus* (55% identity). The alignment of the deduced GL1 amino acid sequence and deduced protein sequences exhibiting high similarity scores is depicted in Figure 4. The highest degree of homology consistently regards the C-terminal part of the deduced proteins.

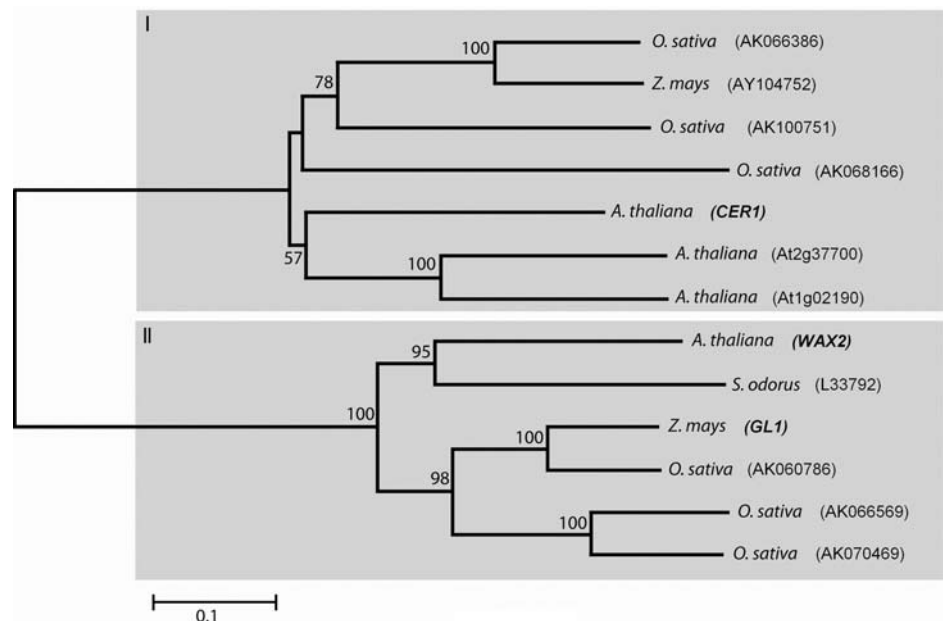
A comparison of the deduced GL1 protein sequence and the product of the Arabidopsis *ECERIFERUM1* (*CER1*) locus, a putative aldehyde decarbonylase active in the cuticular wax biosynthesis pathway, reveals an overall identity of 35%. This similarity score was significantly lower than the degree of similarity encountered between the putative GL1 and Arabidopsis *WAX2* proteins (62%). Since previous results attributed to the maize *GL1* locus a role as an Arabidopsis *CER1* ortholog, we investigated amino acid sequence similarities among a restricted group of *GL1* homolog sequences by means of phylogenetic analysis (Fig. 5). These analyses suggested the presence of two groups of protein sequences, the former containing the *CER1* protein as a founder sequence, the latter including the *WAX2* sequence. Interestingly, the *GL1* sequence showed a high level of homology with the members of the *WAX2* group, while a second maize sequence (GenBank AY104752) was located within the *CER1* group with which it shares 55% amino acid identity. Thus, phylogenetic analysis indicated that *GL1*-related sequences can be divided into two subgroups, each comprising genes from

at least three species: maize, rice, and Arabidopsis (Fig. 5).

### GL1 Transcription Analysis

The 3' end of the *GL1* cDNA was used as a probe in northern-blot experiments performed with total RNA extracted from different tissues of wild-type plants and from leaf tissue homozygous for the *gl1-ref* allele. As shown in Figure 6A, the RNA extracted from wild-type seedlings showed a transcript with an estimated size of 2,300 residues, in accordance with the expected length of the *GL1* mRNA (lane 1). The accumulation of this RNA was dramatically reduced in the *gl1-ref* mutant (lane 2) and was completely blocked in the root where, instead, a transcript of greater size was detected (lane 3). *GL1* expression was evident also in adult leaves (lane 4) and in floral organs (silks and anthers; lanes 5 and 6, respectively), suggesting that *GL1* activity was not restricted to the juvenile developmental phase of the maize plant. The same pattern of hybridization was observed using the complete *GL1* cDNA as a probe (data not shown). To check the amount of RNA loading, the filters were stripped and reprobbed with a maize cytosolic GAPDH clone (Fig. 6B). The *GL1* transcript was further studied by RT-PCR analysis using the samples described above (Fig. 6C). The use of forward and reverse *GL1* primers allowed the amplification of a fragment of the expected size from RNA samples obtained from wild-type seedlings (lane 2) and, at low abundance, from *gl1-ref* mutant leaf (lane 3), mature leaf (lane 5), and anther tissue (lane 7). PCR amplification with primers against cytosolic GAPDH was used to verify the integrity of the samples (Fig. 6D).

**Figure 5.** Phylogenesis of *GL1*-like sequences. The deduced amino acid sequence of the *GL1* locus was aligned against 12 deduced sequences obtained from homologous loci, as available in GenBank. Neighbor-joining analysis was used to obtain a phylogenetic tree, which was bootstrapped over 1,000 cycles. Significance values above a 50% cutoff threshold are indicated near the relative branches. Two distinct groupings are boxed: *CER1*-related sequences (I), including rice AK066386, maize AY104752, rice AK100751, rice AK068166, Arabidopsis At1g02205 (*CER1*), Arabidopsis At2g37700, and Arabidopsis At1g02190; and *WAX2*-related sequences (II), including Arabidopsis At5g57800 (*WAX2*), *S. odorus* L33792, maize AY505017 (*GL1*, this study), rice AK060786, rice AK066569, and rice AK070469. Scale bar, Similarity coefficient.



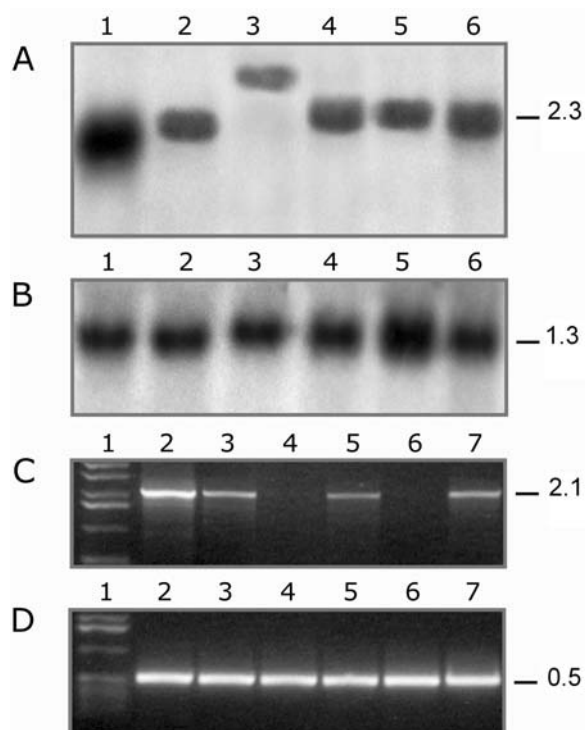


**Figure 6.** Northern analysis and RT-PCR analysis of *GL1* transcription. A, mRNA extracted from young wild-type leaf (1), young *gl1-Ref* leaf (2), root (3), old wild-type leaf (4), silk (5), and anther (6) tissue was hybridized with the 3' end of the *GL1* cDNA. B, The same blot in A was stripped and rehybridized with a GAPDH probe. C and D, The presence of *GL1* (C) and GAPDH (D) transcripts was assayed by RT-PCR in young wild-type leaf (2), young *gl1-ref* leaf (3), root (4), old wild-type leaf (5), silk (6), and anther (7) tissue. Size markers present in lane 1 were used to deduce the sizes of amplification products as indicated on the right.

As can be seen in Figure 6C, from the root (lane 3) and silk (lane 5) extracts no RNA amplification was obtained by RT-PCR. In this respect, we identified an incomplete *GL1*-related clone by screening a silk cDNA library using *GL1* as a probe (H. Hartings, R. Velasco, and M. Motto, unpublished data). This silk cDNA shows 78% identity with *GL1*; northern experiments performed with the same samples as those in Figure 6A give a similar hybridization pattern but with a higher intensity in the silk extract (see Supplemental Fig. 7). This was taken as evidence that a *GL1*-related gene is expressed mainly in the silk tissue and gives rise to an mRNA cross-hybridizing to the *GL1* probe.

As concerns the band in lane 3 of Figure 6A, this might be either a root-specific transcript related in sequence to *GL1* or an unspliced version of *GL1* not amplified by RT-PCR with the conditions used. However, using different combinations of *GL1*-specific primers aimed at identifying the presence of intron sequences in the *GL1* transcript, we had no indication of the occurrence of an unspliced version of the *GL1* mRNA in the root extract (data not shown). Accordingly, this band is likely to be the result of unspecific cross-hybridization.

## DISCUSSION

### Molecular Cloning and Characterization of the *GL1* Locus

To obtain molecular insights into the nature of the genetic lesion that gives rise to the *gl1* phenotype, a collection of unstable *gl1* mutations induced by autonomous elements of the *En/Spm* family was generated (Maddaloni et al., 1990). From one of these mutable alleles, a partial sequence of *GL1* was identified and molecularly cloned, as confirmed by allelic cross-referencing and northern-blot experiments, and used to recover the complete gene from a maize genomic library. *GL1* is a single-copy gene, which gives rise to a transcript carrying a 1,866-bp ORF and spanning eight noncontiguous genomic stretches. The genomic region encompassed by the cDNA sequence includes all the *En* insertion sites found in the unstable *gl1* alleles.

Together, our results indicate that we have cloned the *GL1* genomic sequence and the complete coding region of its major transcript. Hansen et al. (1997), who performed similar experiments to characterize the *GL1* gene, isolated a genomic and a cDNA clone that, according to our results, represent a part of the *GL1* locus and a differently spliced/partial unprocessed mRNA, respectively. Our conclusions are based on several lines of evidence. First, an entire collection of seven independent *En/Spm* insertions was analyzed to define the position of the transposable element in the unstable *gl1* alleles. In four cases, the *En/Spm* insertion sequence is located downstream of the coding region of the *GL1* gene as described by Hansen et al. (1997). Second, the cDNA isolated by Hansen et al. is 1,585 bp long, includes only the first four exons of our cDNA, and codes for a polypeptide of 319 amino acids with homology to CER1 and related proteins limited to the N-terminal region. The C-terminal domain has no counterparts in any of the *GL1* homologs identified so far. Moreover, this polypeptide includes only the first two His-rich motifs. Third, Hansen's clone exactly matches the 5' region of our genomic sequence. Because *GL1* is a single-copy gene, it is concluded that both sequences derive from the same locus. However, the former was isolated by screening a genomic library constructed with *HindIII*-digested DNA. It is likely that the availability of a short *GL1* transcript and the concomitant molecular situation at the *GL1* locus presenting a *HindIII* site in the fourth, relatively lengthy, intron have suggested (Hansen et al., 1997) that the *HindIII* site was located beyond the end of the *GL1* gene. In conclusion, our data regarding the *GL1* transcript, its coding region, and the distribution of *En/Spm* element insertion sites within the locus suggest that the polypeptide described by Hansen et al. is not sufficient to perform the function of the *GL1* gene.

### The *GL1* Gene Encodes a WAX2-Related Protein Displaying Transmembrane Domains

The putative protein encoded by *GL1* is 621 amino acids long and is related in length and sequence to those coded by a number of loci from different plant species. These polypeptide sequences display several predicted transmembrane domains in the N-terminal region and a globular domain in the C-terminal part. A common feature shared by these proteins is the presence of eight conserved His motifs in the tripartite domain H-X<sub>2,4</sub>-H, H-X<sub>2,3</sub>-H-H, (H/Q)-X<sub>2,3</sub>-H-H, which form a di-iron-binding site essential for catalytic activity in a large family of integral membrane enzymes, such as acyl desaturases, alkyl-hydroxylases, epoxydases, acetylenases, methyl oxidases, ketolases, and decarboxylases, activities found in prokaryotes and eukaryotes (Shanklin and Cahoon, 1998, and refs. therein). The *GL1*-related proteins identified by means of sequence comparisons include the *WAX2* and *CER1* gene products of Arabidopsis, both of which are involved in cuticular wax production. Interestingly, in the *GL1*, *WAX2*, and *CER1* genes, intron positions are conserved (see Supplemental Fig. 8), suggesting a common origin from the same ancestor gene. However, *GL1* shows 62% overall amino acid identity to *WAX2*, which rises to 78% when the C-terminal region is considered, compared to 35% homology with *CER1*. Therefore, *GL1* is probably the *WAX2* ortholog from maize. In addition, sequence comparison clearly indicates the presence of two distinct subgroups of *GL1*-related genes in rice, maize, and Arabidopsis. The former, including *GL1* itself, is related to the *WAX2* gene of Arabidopsis, while the latter comprises sequences more similar to *CER1*, among which is a maize expressed sequence tag (EST; ID AY104752; see Fig. 5), which could be the true *CER1* ortholog of maize.

Mutations of *GL1*, *CER1*, and *WAX2* cause dramatic alterations in composition and crystallization patterns of cuticular waxes (Lorenzoni and Salamini, 1975; Bianchi et al., 1985; Jenks et al., 1995; Chen et al., 2003). Cuticular wax of juvenile maize leaves is composed of primary alcohols (63%), aldehydes (20%), and esters (16%) mainly derived from C32 acyl moieties, whereas on Arabidopsis stems the main constituents are alkanes (53%) and ketones (23%), with primary alcohols and aldehydes reduced to 11% and 4%, respectively. Arabidopsis leaves are almost devoid of ketones, and alkanes represent 72% of total waxes. Because of these differences in wax composition, comparing the biochemical effect of *wax* gene mutations in maize and Arabidopsis is not conclusive in defining the homology in gene functions.

*CER1* was suggested to be an aldehyde decarboxylase because the mutant shows an increase in aldehydes and a reduction of the products of aldehyde decarboxylation, namely, alkane, secondary alcohols, and ketones (Aarts et al., 1995). In maize, these latter compounds represent only 1% of total cuticular waxes; therefore, mutations in a putative aldehyde decarboxylase are not likely to be identified based only on visual screenings.

ylase are not likely to be identified based only on visual screenings.

In *wax2* mutants, total wax load is diminished by about 80% because of the reduced accumulation of all the prevalent wax constituents, including aldehydes, with the exception of C30 primary alcohols, which are increased on *wax2* stems.

Wax load on *gl1* juvenile leaves is reduced by 73% compared to the wild type due to a decreased accumulation of both aldehydes and primary alcohols, while the amount of esters does not change. The mutation has a pronounced effect on the synthesis of long-chain wax compounds (C32), whereas those with shorter acyl chains are less affected or even increased (Bianchi et al., 1977). The overall change in wax composition on *gl1* seedlings is similar to that observed on *wax2* mutant leaves. In conclusion, these biochemical data on composition of mutant waxes also support the conclusion that *GL1* is more closely related to *WAX2* than to *CER1*.

### The *gl1* Mutation Affects Cuticular Wax Accumulation and Other Cuticular Traits

The Arabidopsis *WAX2/YRE* gene described by Chen et al. (2003) and Kurata et al. (2003) has a broad role in cuticle biosynthesis. Its mutation alters both cutin morphology and wax production. In addition, this mutation affects other cuticular and plant traits, including trichome development, leaf transpiration, pollen fertility, and postgenital organ fusion during early organ development. Similarly to *wax2*-defective plants, *gl1-ref* mutants display a reduction in cuticular wax deposition and alterations in cuticle membrane structure and trichome development. However, postgenital organ fusion was not observed in the *gl1-ref* mutant. As a possible explanation for these discrepancies, the *gl1-ref* allele might condition a leaky mutation impairing only some of the *GL1* functions. However, a null-transcript *gl1* mutant shows normal development and the absence of organ fusion (data not shown). A second possible explanation is the different effect of the two mutations on cutin morphology, which could be of functional importance: In *wax2* mutants, cuticle membrane thickness is increased, although its weight is reduced.

Alternatively, different roles on plant development may be ascribed to maize and Arabidopsis cuticles. In addition to *wax2*, the *abnormal leaf shape1* (*ale1*) and *lacerata* (*lcr*) Arabidopsis mutants are altered in cuticle membrane morphology and display postgenital organ fusion (Tanaka et al., 2001; Wellesen et al., 2001). Instead, the *long-chain acyl-CoA synthetase2* (*lacs2*) mutant shows a reduction in cutin thickness (−40%) and several phenotypic alterations normally associated with defective cutin structure but not organ fusion, suggesting that this trait is very likely linked to more drastic cutin impairments (Schnurr et al., 2004). The causal relationship between cuticle membrane defects and postgenital organ fusion in Arabidopsis is

strengthened by the finding that degradation of the cutin layer in transgenic *Arabidopsis* plants expressing a cutinase gene leads to adhesion of different adult organs (Sieber et al., 2000).

A similar correlation is not observed in maize and other monocots. Maize mutants with adhesion-competent epidermal cells include *crinkly4* (*cr4*) and *adherent1* (*ad1*). The *cr4* mutation has a broad effect on epidermal cell morphology, not restricted to the cuticular layer (Becraft et al., 1996). *ad1* mutants exhibit alteration in cell wall structure and epicuticular wax deposition in the epidermal layer, while the cuticle membrane in adherent regions appears intact (Sinha and Lynch, 1998). By contrast, the sorghum *bm-22* mutant with a severely reduced cuticle membrane displays normal plant structure and development (Jenks et al., 1994). Moreover, maize seedlings treated with an inhibitor of cutin synthesis have no visual phenotypic alterations (Lequeu et al., 2003). Collectively, these results point to a different role of maize and *Arabidopsis* cuticles in plant development, namely, in the prevention of postgenital organ fusion.

### Expression of the *GL1* Gene Is Tissue and Organ Specific and Developmentally Regulated

As far as *GL1* function is concerned, analysis of the mutant phenotype indicates that *GL1*, like the other *GLOSSY* genes, is an essential component of the juvenile wax layer biosynthetic route (Bianchi et al., 1985). Young *gl1* leaves have the chemical wax composition of wild-type adult leaves. It can be concluded that the regulation of *GL1* expression is an integral part of the cell response to age-related events of differentiation. It was shown that in maize the juvenile-to-adult transition is under genetic control, with a series of independent mutations—*CORN-GRASS1* (*CG1*), *TEOPOD1* (*TP1*), *TEOPOD2* (*TP2*), *HAIRY-SHEATH-FRAYED1* (*HSF1*; Poethig, 1988, and refs. therein), and *GL15* (Moose and Sisco, 1996)—altering the transition from juvenile to adult vegetative growth. The interaction of *GL15* with *TP1* and *TP2* indicates that *GL15* acts downstream of these genes and that it is required for their effect during epidermis development (Evans et al., 1994). The *GL15* gene is a transcriptional activator of the *APETALA2* family of regulatory genes (Moose and Sisco, 1996), which is expected to interact directly with the promoters of structural genes needed for the accumulation of cuticular waxes, a prediction that can be experimentally tested now that *GL1*, *GL2*, and *GL8* are listed among the cloned genes contributing to wax deposition.

From the expression profile experiments, it can be argued that the regulation of the expression of the characterized *GLOSSY* genes is more complex than predicted only on the basis of seedling phenotypes. *GL8* turns out to be expressed in different organs of the adult plant, including the roots, although to a lesser extent than in seedling leaves (Xu et al., 1997). *GL1* is not expressed in the root but is detectable in anthers

and, to a minor extent, also in adult leaves, similar to the *GL2* transcript that, besides being characteristically produced in young leaves, is also detectable in the part of the maize shoot contributing to the development of the female inflorescence (Velasco et al., 2002). These results demonstrate that the *GL1* protein, like the products of other *GLOSSY* genes, is not merely involved in the cuticle formation of the green part of the maize seedling. Together, these findings indicate that factors conditioning tissue juvenility may be reactivated after the formation of the lateral meristem (Uhrig et al., 1997). Alternatively, a different control mechanism affecting wax biosynthetic genes should exist in adult plant tissues.

## MATERIALS AND METHODS

### Plant Material

The origin and maintenance of the *wx-m7* transposon stock, the *gl1-ref* allele used in this study, and the recovery of the *gl1*-mutable strains have been described previously (Maddaloni et al., 1990). Briefly, *gl1* alleles were identified in the F<sub>1</sub> generation of a cross between a strain homozygous for the unstable allele *wx-m7* of the *WAXY* locus and for a dominant *GL1* allele (used as the male parent) and a female parent strain homozygous for the stable recessive *gl1-ref* allele. Both strains were in the Wf9 inbred line genetic background. The instability of the *wx-m7* allele is due to the transposable element *Ac* (McClintock, 1962; Behrens et al., 1984). In our tagging experiments, nine unstable alleles were generated at the *GL1* locus. Seven, *gl1-m1*, 2, 3, 5, 7, 8, and 9, were due to the insertion of an autonomous element, while *gl1-m4* and *gl1-m6* were caused by a nonautonomous element of a family of transposable elements different from *Ac/Ds* (Maddaloni et al., 1990).

The *wx-m7* stock also contains copies of active autonomous *En/Spm* elements (Michel et al., 1995). To test for the presence in *gl1-m5* in stable mutants of *En/Spm* elements, crosses with two tester strains were generated. The resulting F<sub>1</sub> plants were selfed and the F<sub>2</sub> seeds were checked for mutability of either of the two tester alleles, *a1-m(r)* or *a1-m1*, both due to the insertion of a defective *En/Spm* element (*I/dSpm*) and showing somatic instability only in the presence of an active *En/Spm* element. In its absence, the *a1-m1* allele gives rise to kernels with a pale color, while *a1-m1(r)* is colorless. In the presence of an active *En/Spm* element, colored spots are produced on the pale (*a1-m1*) or colorless [*a1m(r)*] background. Crosses and selfings were according to standard procedures.

### Genomic Cloning and Southern Analysis

Maize (*Zea mays*) DNA was isolated from leaves of flowering plants or from seedlings as described (Michel et al., 1995). Southern hybridizations and radioactive labeling of probes were according to standard procedures (Sambrook et al., 1989). A plasmid clone carrying the complete *En/Spm* element isolated from the *wx-844* allele was provided by Dr. Alfons Gierl (Munich). An *EcoRI/BamHI* restriction fragment that covered the internal region of the *En/Spm* element between positions 2,518 to 4,459 (Pereira et al., 1986) was used as a molecular probe.

Southern analysis was performed to map the position of the *En* element in seven unstable *gl1* alleles. For this purpose, genomic DNA from homozygous mutant plants was digested with the restriction enzymes *BamHI*, *HindIII*, *ApaI*, *SstI*, *SpeI*, and *KpnI*. Blots were probed with four PCR-derived fragments of the *GL1* allele covering regions (base positions are indicated relative to the translation start site) from -2,302 to -648 (probe I), from +1,213 to +2,048 (probe II), from +2,426 to +3,581 (probe III), and from +4,131 to +4,745 (probe IV).

*HindIII*-digested genomic fragments from 7 to 11 kb from plants carrying the *gl1-m5* allele were cloned into the  $\lambda$ EMBL3 vector, after separation and purification from agarose gels with the QIAEX gel extraction kit (Qiagen, Valencia, CA). Nine clones hybridizing to a fragment covering the *En/Spm* sequence between the *EcoRI* sites at positions 5,836 and 8,278 were identified within approximately 100,000 recombinant phages. Restriction mapping of

the clones identified a single clone, designated  $\lambda$ -09, carrying a *Hind*III insert of approximately 8.3 kb, which was chosen for further analysis.

Recombinant clones carrying a wild-type *GL1* allele were recovered from a maize BAC library derived from DNA extracted from the inbred F<sub>2</sub>, kindly provided by Dr. Keith Edwards (University of Bristol, UK).

## Northern and RT-PCR Analysis

Total RNA was isolated from the following organs and tissues of the inbred Wf9: second and third leaf of wild-type and *gl1-ref* mutant seedlings, wild-type roots of 1-week-old seedlings, wild-type adult leaf (top leaf, surrounding the tassel), wild-type silks, and wild-type anthers (both immature and pollen-shedding, from the same tassel). Extractions were performed using TRIzol (Invitrogen, Carlsbad, CA) according to the manufacturer's instructions. For northern experiments, 20  $\mu$ g of total RNA samples were fractionated on denaturing gels, capillary blotted onto nylon membranes (Hybond N+; Amersham, Little Chalfont, UK), and hybridized at 45°C in UltraHyb solution (Ambion, Austin, TX). Filters were washed at 55°C in 2 $\times$  SSC/0.1% SDS (15 min), in 1 $\times$  SSC/0.1% SDS (30 min), and in 0.1 $\times$  SSC/0.1% SDS (30 min). RNA markers from 0.2 to 10 kb (Sigma-Aldrich, St. Louis) were used as size standards. Probes were the full-length *GL1* cDNA and the 400-bp 3' end, including the complete 3' UTR, of a partial *GL1* clone isolated from a seedling cDNA library. To check the amount of RNA loading, filters were rehybridized with a probe derived from maize cytosolic GAPDH cDNA.

For RT-PCR, 5  $\mu$ g of total RNA were reverse transcribed using SuperScriptII reverse transcriptase (Invitrogen) according to manufacturer's instructions. One-twentieth of the final reaction product was amplified by PCR with the following primers: forward, 5'-ATCGAATTCACGTACGG-CACAGTTGCTAGC-3'; reverse, 5'-CGCTCTAGACCACCAATTCACACTC-GACG-3'.

The forward primer annealed to the region of the *GL1* cDNA starting 70 bp upstream of the ATG start codon, while the reverse primer annealed to the region starting 101 bp downstream of the stop codon. To avoid formation of secondary structures, PCR reactions were performed in the presence of 10% DMSO (final concentration). The 5' end of the forward and reverse primers included, respectively, *Eco*RI and *Xba*I restriction sites (indicated in italics in the above sequences), which were used to subclone the *GL1* cDNA from leaves of the inbred Wf9 into the pBluescriptSKII vector (Stratagene, La Jolla, CA) prior to sequencing. Five independent clones were sequenced on both strands to determine the sequence of the *GL1* cDNA.

## DNA Sequencing

DNA sequencing was carried out with an automatic sequencer (CEQ 8000; Beckman-Coulter, Fullerton, CA). Genomic and cDNA sequences were determined on both strands.

## Microscopic Inspection

SEM was used to study adaxial surfaces of primary leaves of *gl1* mutant and wild-type plants grown for 2 to 3 weeks in a phytochamber at 26°C/19°C (day/night) and 40% humidity with a 16/8-h light/dark rhythm, and a light intensity of 1,900  $\mu$ E m<sup>-2</sup> s<sup>-1</sup>. Segments of the middle part of the leaf blade were fixed to a specimen holder by tissue tek and shock frozen with liquid nitrogen within a high vacuum cryo preparation stage. Samples were transferred under vacuum to a cryo preparation chamber where they were sputter coated with gold and examined on the cold stage of a Zeiss DSM 940 SEM (Carl Zeiss NTS GmbH, Oberkochen, Germany). For TEM investigation of the cuticle, small pieces (2–3 mm<sup>2</sup>) of primary leaf blades were fixed for 2 h at room temperature in 2.5% (v/v) glutaraldehyde and 2% (v/v) formaldehyde in 0.05 M phosphate buffer (PB), pH 6.8. After washing in PB, samples were postfixed for 1 h in 2% (v/v) osmium tetroxide in PB, washed again, and dehydrated through a graded series of ethanol. Samples were then infiltrated with LR White resin (Plano, Marburg, Germany) and polymerized for 48 h at 60°C. Ultrathin cross-sections were prepared and mounted on carbon-coated Formvar copper grids (200 mesh; Plano). After staining with 2% uranyl acetate for 2 h, sections were inspected with a Zeiss EM 10 TEM (Carl Zeiss NTS GmbH).

## Statistical Analysis

Multiple DNA and protein sequence alignments were performed using ClustalW (Thompson et al., 1994), while phylogenetic analysis was performed according to the MEGA version 2.1 software package (Kumar et al., 2001). For tree construction based on aligned amino acid sequences, the neighbor-joining tree-building method was utilized. Bootstrap analysis (1,000 replicates) was used to assign a consensus tree at a 50% cutoff value.

Sequence data from this article have been deposited with the EMBL/GenBank data libraries under accession numbers AY505017 and AY505498.

## ACKNOWLEDGMENT

We thank Dr. Keith Edwards, University of Bristol, UK, for providing a recombinant BAC clone carrying a wild-type *GL1* gene.

Received December 15, 2004; returned for revision February 9, 2005; accepted February 9, 2005.

## LITERATURE CITED

- Aarts MGM, Keijzer CJ, Stiekema WJ, Pereira A (1995) Molecular characterization of the *CER1* gene of Arabidopsis involved in epicuticular wax biosynthesis and pollen fertility. *Plant Cell* 7: 2115–2127
- Becraft PW, Stinard PS, McCarty DR (1996) CRINKLY4: a TNFR-like receptor kinase involved in maize epidermal differentiation. *Science* 273: 1406–1409
- Behrens U, Federoff N, Laird A, Müller-Neumann M, Starlinger P, Yoder J (1984) Cloning of the *Zea mays* controlling element *Ac* from the *wx-m7* allele. *Mol Gen Genet* 194: 346–347
- Bianchi A, Bianchi G, Avato P, Salamini F (1985) Biosynthetic pathways of epicuticular wax of maize as assessed by mutation, light, plant age and inhibitor studies. *Maydica* 30: 179–198
- Bianchi G, Avato P, Salamini F (1977) *glossy* mutants of maize. VII. Chemistry of *glossy1*, *glossy3* and *glossy7* epicuticular waxes. *Maydica* 22: 9–17
- Chen X, Goodwin SM, Boroff VL, Liu X, Jenks MA (2003) Cloning and characterization of the *WAX2* gene of Arabidopsis involved in cuticle membrane and wax production. *Plant Cell* 15: 1170–1185
- Evans M, Passas HJ, Poethig RS (1994) Heterochronic effects of *glossy15* mutations on epidermal cell identity in maize. *Development* 120: 1971–1981
- Hansen JD, Pyee J, Xia Y, Wen T-J, Robertson DS, Kolattukudy PE, Nikolau BJ, Schnable PS (1997) The *glossy1* locus of maize and an epidermis-specific cDNA from *Kleberia odorata* define a class of receptor-like proteins required for the normal accumulation of cuticular waxes. *Plant Physiol* 113: 1091–1100
- Jenks MA, Joly RJ, Peters PJ, Rich PJ, Axtell JD, Ashworth EN (1994) Chemically induced cuticle mutation affecting epidermal conductance to water vapor and disease susceptibility in *Sorghum bicolor* (L.) Moench. *Plant Physiol* 105: 1239–1245
- Jenks MA, Tuttle HA, Eigenbrode SD, Feldmann KA (1995) Leaf epicuticular waxes of the *eceriferum* mutants in Arabidopsis. *Plant Physiol* 108: 369–377
- Kolattukudy PE (1996) Biosynthetic pathways of cutin and waxes and their sensitivity to environmental stresses. In G Kerstiens, ed, *Plant Cuticles*. BIOS Scientific Publishers, Oxford, pp 83–108
- Kumar S, Tamura K, Jakobsen IB, Nei M (2001) MEGA2: molecular evolutionary genetics analysis software. *Bioinformatics* 17: 1244–1245
- Kunst L, Samuels AL (2003) Biosynthesis and secretion of plant cuticular waxes. *Prog Lipid Res* 42: 51–80
- Kurata T, Kawabata-Awai C, Sakuradani E, Shimizu S, Okada K, Wada T (2003) The *YORE-YORE* gene regulates multiple aspects of epidermal cell differentiation in Arabidopsis. *Plant J* 36: 55–56
- Lawson EJR, Poethig RS (1995) Shoot development in plants: time for a change. *Trends Genet* 11: 263–268
- Lequeu J, Fauconnier M-L, Chammai A, Bronner R, Blée E (2003) Formation of plant cuticle: evidence for the occurrence of the peroxyl-gene pathway. *Plant J* 36: 155–164

- Lorenzoni C, Salamini F** (1975) *glossy* mutants of maize. V. Morphology of the epicuticular waxes. *Maydica* **20**: 5–19
- Maddaloni M, Bossinger G, Di Fonzo N, Motto M, Salamini F, Bianchi A** (1990) Unstable alleles of the *Glossy1* locus of maize show a light-dependent variation in the pattern of somatic reversion. *Maydica* **35**: 409–420
- McClintock B** (1962) Aspects of gene regulation in maize. *Carnegie Inst Wash Year Book* **63**: 592–603
- Michel D, Hartings H, Lanzini S, Michel M, Motto M, Riboldi GR, Salamini F, Döring H-P** (1995) Insertion mutations at the maize *Opaque2* locus induced by transposable element families *Ac*, *En/Spm*, and *Bg*. *Mol Gen Genet* **248**: 287–292
- Moose SP, Sisco PH** (1994) *Glossy15* controls the epidermal juvenile-to-adult phase transition in maize. *Plant Cell* **6**: 1343–1355
- Moose SP, Sisco PH** (1996) *Glossy15*, an *APETALA2*-like gene from maize that regulates leaf epidermal cell identity. *Genes Dev* **10**: 3018–3027
- Neuffer M, Coe E, Wessler SR** (1997) *Mutants in Maize*. Cold Spring Harbor Laboratory Press, Cold Spring Harbor, NY
- Pereira A, Cuypers H, Gierl A, Schwarz-Sommer Z, Saedler H** (1986) Molecular analysis of the *En/Spm* transposable element system of *Zea mays*. *EMBO J* **5**: 835–841
- Poethig RS** (1988) Heterochronic mutations affecting shoot development in maize. *Genetics* **119**: 959–973
- Post-Beittenmiller D** (1996) Biochemistry and molecular biology of wax production in plants. *Annu Rev Plant Physiol Plant Mol Biol* **47**: 405–430
- Sambrook J, Fritsch EF, Maniatis T** (1989) *Molecular Cloning: A Laboratory Manual*, Ed 2. Cold Spring Harbor Laboratory Press, Cold Spring Harbor, NY
- Schnurr J, Shockey J, Browse J** (2004) The acyl-CoA synthetase encoded by *LACS2* is essential for normal cuticle development in Arabidopsis. *Plant Cell* **16**: 629–642
- Shanklin J, Cahoon EB** (1998) Desaturation and related modifications of fatty acids. *Annu Rev Plant Physiol Plant Mol Biol* **49**: 611–641
- Sieber P, Schorderet M, Ryser U, Buchala A, Kolattukudy P, Metraux JP, Nawrath C** (2000) Transgenic Arabidopsis plants expressing a fungal cutinase show alterations in the structure and properties of the cuticle and postgenital organ fusions. *Plant Cell* **12**: 721–737
- Sinha N, Lynch M** (1998) Fused organs in the *adherent1* mutation in maize show altered epidermal walls with no perturbations in tissue identities. *Planta* **206**: 184–195
- Tacke E, Korfhage C, Michel D, Maddaloni M, Motto M, Lanzini S, Salamini F, Döring H-P** (1995) Transposon tagging of the maize *Glossy2* locus with the transposable element *En/Spm*. *Plant J* **8**: 907–917
- Tanaka H, Onouchi H, Kondo M, Hara-Nishimura I, Nishimura M, Machida C, Machida Y** (2001) A subtilisin-like serine protease is required for epidermal surface formation in Arabidopsis embryos and juvenile plants. *Development* **128**: 4681–4689
- Thompson JD, Higgins DG, Gibson TJ** (1994) CLUSTAL W: improving the sensitivity of progressive multiple sequence alignment through sequence weighting, position-specific gap penalties and weight matrix choice. *Nucleic Acids Res* **22**: 4673–4680
- Uhrig H, Marocco A, Döring H-P, Salamini F** (1997) The clonal origin of the lateral meristem generating the ear shoot of maize. *Planta* **201**: 9–17
- Velasco R, Korfhage C, Salamini A, Tacke E, Schmitz J, Motto M, Salamini F, Döring H-P** (2002) Expression of the *glossy2* gene of maize during plant development. *Maydica* **47**: 71–81
- Walton TJ** (1990) Waxes, cutin and suberin. In JL Harwood, JR Bowyer, eds, *Methods in Plant Biochemistry: Lipids, Membranes and Aspects of Photobiology*. Academic Press, San Diego, pp 105–158
- Wellersen K, Durst E, Pinot F, Benveniste I, Nettekheim K, Wisman E, Steiner-Lange S, Saedler H, Yephremov A** (2001) Functional analysis of the *LACERATA* gene of Arabidopsis provides evidence for different roles of fatty acid  $\omega$ -hydroxylation in development. *Proc Natl Acad Sci USA* **98**: 9694–9699
- Xu X, Dietrich CR, Delledonne M, Xia Y, Wen T-J, Robertson DS, Nikolau BJ, Schnable PS** (1997) Sequence analysis of the cloned *glossy8* gene of maize suggests that it may code for a  $\beta$ -ketoacyl reductase required for the biosynthesis of cuticular waxes. *Plant Physiol* **115**: 501–510
- Xu X, Dietrich CR, Lessire R, Nikolau BJ, Schnable PS** (2002) The endoplasmic reticulum-associated maize GL8 protein is a component of the acyl-coenzyme A elongase involved in the production of cuticular waxes. *Plant Physiol* **128**: 924–934